Low-frequency dynamics in superionic borate glasses by coupled Raman and inelastic neutron scattering

A. Fontana
Dipartimento di Fisica dell'Università degli Studi di Trento, I-38050 Povo (Trento), Italy and Unità di Trento, Centro Interuniversitario di Struttura della Materia del Ministero della Pubblica Istruzione e Gruppo Nazionale di Struttura della Materia del Consiglio Nazionale delle Ricerche, I-38050 Povo (Trento), Italy

F. Rocca
Centro di Fisica degli Stati Aggregati ed Impianto Ionico del Consiglio Nazionale delle Ricerche, I-38080 Povo (Trento), Italy and Unità di Trento, Centro Interuniversitario di Struttura della Materia del Ministero della Pubblica Istruzione e Gruppo Nazionale di Struttura della Materia del Consiglio Nazionale delle Ricerche, I-38050 Povo (Trento), Italy

M. P. Fontana and B. Rosi
Dipartimento di Fisica dell'Università degli Studi di Parma, via Massimo D'Azeglio 85, I-43100 Parma, Italy and Unità di Parma, Centro Interuniversitario di Struttura della Materia del Ministero della Pubblica Istruzione e Gruppo Nazionale di Struttura della Materia del Consiglio Nazionale delle Ricerche, I-43100 Parma, Italy

A. J. Dianoux
Institute Max Laue–Paul Langevin, Boîte Postale 156X, 38042 Grenoble CEDEX, France
(Received 24 July 1989)

We report a study of low-frequency vibrational dynamics and electron-vibration coupling in AgI-doped silver borate glasses, which have been shown to have anomalies which could be connected to microscopic fractality. By using both Raman scattering and time-of-flight neutron-scattering spectroscopies, we were able to determine the vibrational density of states and, for the first time in a fractal system, the frequency dependence of the electron-vibration coupling function $C(\omega)$. The results confirm the microscopic fractality of this system. In particular the fracton dimensionality was determined to be 1.4, and a scaling law behavior of $C(\omega)$ was confirmed.

I. INTRODUCTION

Perhaps the most interesting consequences of fractality[1] in microscopic systems are dynamical anomalies in vibrational-diffusive motions or in relaxation processes.[2] In spite of much theoretical work on the subject,[3] to date no direct experimental determination of scaling behavior in a relaxation function has appeared in the literature. In this paper we wish to present such determination for the case of the electron-vibration coupling function in the superionic borate glass $(AgI)_x(Ag_2O\cdot B_2O_3)_{1-x}$.

In a previous paper,[4] dynamical evidence was presented for microscopic fractality in this system, and the deduction was made that AgI dissolved in the glassy borate matrix in the form of a three-dimensional percolation network, containing both the infinite and finite clusters of AgI tetrahedra. The evidence was obtained by Raman spectroscopy, and thus had the drawback that the observed spectral density contained not only the vibrational density of states $g(\omega)$ but also the electron-vibration coupling function $C(\omega)$. Since this latter function was unknown, some reasonable functional form had to be *assumed* in order to obtain $g(\omega)$, and this weakened the general conclusions on the fractality of the system and the determination of the fracton (or spectral) dimensionality $\tilde{d}$ from the frequency dependence of the reduced Raman spectral density $I_R(\omega)$. What was needed was an independent determination of $g(\omega)$.

In this paper we present data obtained by both Raman and inelastic neutron-scattering spectroscopy taken on the same samples of the $(AgI)_x(Ag_2O\cdot B_2O_3)_{1-x}$ system. From neutron scattering it is possible to obtain a "neutron-weighed" vibrational density of states $g_N(\omega)$ which should be reasonably close to the true vibrational density of states $g(\omega)$.

Determinations of this type, which show an anomalous frequency dependence of $g(\omega)$ which could be related to some kind of fractality, have already appeared in the literature for the case of water,[5] diglycidyl ether of bisphenol *A* DGEB*A*, a constituent of epoxy resins,[6] and silica smoke-particle aggregates.[7] However, no coupled Raman neutron-scattering measurement was performed, and therefore only the fracton dimensionality could be deduced. In this paper we determine instead not only $\tilde{d}$ but also the scaling behavior of the electron-vibration coupling in a system which our data confirm to show dynamical fractality. As we shall see, $C(\omega)$ may be easily obtained from the ratio of the reduced Raman intensity $I_R(\omega)$ and $g_N(\omega)$.

Our results confirm the conclusions of Ref. 4, and in particular the assumption (see also Duval *et al.*[3]) made for the scaling behavior of $C(\omega)$ is verified nicely by the experiment reported here.

II. EXPERIMENTAL PROCEDURES AND DATA ANALYSIS

A. Sample preparation

Disk-shape samples (50-mm diameter, 2-mm thickness) were prepared in our laboratory following the standard procedure.[8] We used special grade AgI and $AgNO_3$ from Erba (Italy). The ^{11}B-enriched B_2O_3 was supplied by Centronic Limited (England) and certified as 97% ^{11}B. In order to allow a complete reduction of $AgNO_3$ to Ag_2O, the powders were at first heated in a quartz crucible to 700 K for 2 h. Melting was achieved by further heating to 800 K for 5 h. Quenching was obtained by rapidly pouring and pressing the melted compound into a circular steel mould kept at 100–150 °C. The sample was then annealed at $T < T_g$ (glass temperature) in order to minimize thermal stresses.

Chemical analysis, T_g, and density measurements gave results in agreement with those obtained by similar procedures by other authors.[8] No evidence of any crystalline structure was found by x-ray diffraction measurements performed on the same samples utilized for scattering measurements.

B. Raman scattering

We have performed light-scattering measurements at low frequency on superionic borate glasses $(AgI)_x(Ag_2O{\cdot}B_2O_3)_{1-x}$ as a function of the AgI content $(0.50 < x < 0.70)$. The measurements have been performed with a standard system in vh (depolarized) and vv (polarized) configurations. We used the 6471-Å krypton laser line at a nominal power level which was always kept below 50 mW in order to avoid undue heating of the sample. The spectra were taken down to 3 cm^{-1} with a spectral bandpass of 0.8 cm^{-1}. A slowly varying luminescence background was parametrized and then subtracted from the scattered intensity.

Previous measurements[9] performed at room temperature showed a strong "quasielastic" contribution at the lowest frequencies. Such scattering was attributed to a polarizability relaxation due to the jumps of the Ag^+ ions in the available sites of the host matrix. Because of the clearly different nature of the extra scattering and the phonon scattering, the first was subtracted out. In any case, the extra scattering is strongly dependent on temperature (see Fig. 1) and at low temperature it is negligible in the frequency range available to our double monochromator. For this reason the Raman measurements were performed mainly at low temperature (80 K).

In order to compare the Raman data to the neutron data, it is convenient to use the reduced Raman intensity[10]

$$I_R(\omega)=I(\omega)\frac{\omega}{n(\omega,T)+1}\ , \tag{1}$$

where $n(\omega,T)$ is the Bose-Einstein statistical factor and $I(\omega)$ is the experimental Raman spectrum.

For an isotropic disordered solid, the electronic transition polarizability contains only two independent quantities: the diagonal elements P_{vv} and the off-diagonal elements P_{vh}. These two quantities are probed in the usual 90° scattering experiment, where $vv(h)$ stands for the geometry in which the incident and scattered electric fields are parallel (perpendicular).

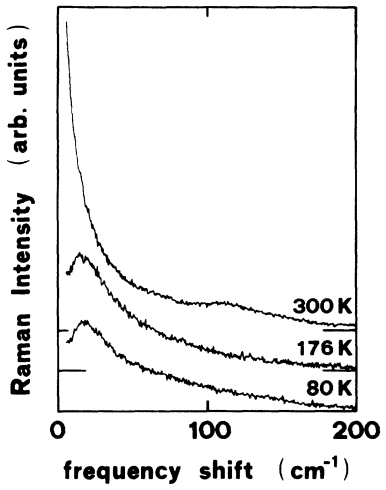

FIG. 1. Temperature dependence of low-frequency Raman scattering of $x = 0.65$ sample.

Using this notation, the reduced Raman intensity is given by[11]

$$I_R(\Omega_0,\omega)=\frac{(\Omega_0+\omega)^4}{2\pi c^3}\hbar V E_0^2\sum_b C_b(\Omega_0,\omega)g_b(\omega)\ , \tag{2}$$

where Ω_0 is the frequency of the incident light, ω is the Raman shift, E_0 is the incident electric field amplitude, V is the scattering volume, b indicates the acoustic and optic bands, and $g_b(\omega)$ is the corresponding density of states. The electron-vibration coupling is given by

$$C_b(\omega)=\left|\sum_l P^l u_l(\omega)\right|^2\ , \tag{3}$$

where only first-order terms of the expansion of the electronic polarizability tensor as a function of the displacement eigenvectors $u_l(\omega)$ have been retained. In (3) the Ω_0 dependence of C_b was dropped since we assume off-resonance conditions. In the low-frequency acoustic region we assume $C_b(\omega)=C_{ac}(\omega)\equiv C(\omega)$ and $g_b(\omega)=g_{ac}(\omega)\equiv g(\omega)$.

The correct evaluation of $C(\omega)$ is an open problem because it depends on many physical properties which differ for different systems. On general grounds, however, we should expect that in the acoustic-phonon range $C(\omega)\approx\omega^2$, but only few experiments have confirmed this assumption:[12] furthermore, at very low frequencies the Raman spectra of many amorphous systems show the so-called "extra scattering," which in many cases is also temperature dependent; this makes it difficult to check the ω^2 dependence down to the Brillouin shift range. Thus in this paper we prefer to treat $C(\omega)$ as a phenomenological quantity to be determined experimentally by comparing the Raman data with the neutron data.

C. Neutron scattering

For a system of identical atoms of mass M, the one-phonon incoherent neutron differential scattering cross section is given by[13]

$$\frac{d^2\sigma_{\rm inc}}{d\Omega\, d\omega}=\frac{k}{k_0}b_{\rm inc}^2\exp\left[-\frac{\hbar\omega}{2k_BT}\right]\tilde{S}_s(Q,\omega)\ , \tag{4}$$

where $\mathbf{Q}=k-k_0$ is the momentum transfer (k_0 and k being the incident and scattered neutron wave vectors, respectively), $\hbar\omega$ is the energy exchange, $b_{\rm inc}$ is the incoherent scattering length, and $\tilde{S}_s(Q,\omega)$ is the symmetrized scattering law. Using the reduced variables[14]

$$\alpha=\frac{\hbar^2Q^2}{2Mk_BT}\ ,$$

$$\beta=\frac{\hbar\omega}{k_BT}\ ,$$

the scattering law may be written as

$$\tilde{S}_s(\alpha,\beta)=e^{-Q^2\langle u^2\rangle}\frac{\alpha}{2\beta\sinh(\beta/2)}g(\omega)\ . \tag{5}$$

The generalized frequency distribution is defined as

$$P(\alpha,\beta)=2\beta\sinh(\beta/2)\frac{\tilde{S}_s(\alpha,\beta)}{\alpha}\ . \tag{6}$$

The standard procedure to obtain the density of states $g(\omega)$ consists of an extrapolation of the function P for α (i.e., Q) tending to zero[14]

$$g(\omega)=2\beta\sinh(\beta/2)\lim_{\alpha\to0}\left[\frac{\tilde{S}_s(\alpha,\beta)}{\alpha}\right]\ , \tag{7}$$

where the coherent contributions to the experimental scattering law are eliminated by the extrapolation to zero exchanged momentum. However, this procedure neglects the multiphonon contribution to the scattering, which in many cases may be important, especially at high temperatures.

Things become much more complicated in the more general case of a polyatomic formula unit, with n atoms of species i, concentration c_i, and scattering cross section $\sigma_i^{\rm inc}=4\pi b_{i,\rm inc}^2$ in the unit cell. In this case we may define a *neutron-weighed* density of states:

$$g_N(\omega)=\frac{\overline{M}}{\overline{\sigma}}\sum_{i=1}^{n}c_i\frac{\sigma_i}{m_i}g_i(\omega)\ , \tag{8}$$

where $\overline{M}$ is the average atomic mass and σ the average atomic cross section. Such a quantity is as close as possible to an experimental determination of the true density of states of a polyatomic system. In our case, as we shall see, in the low-frequency range $g_N(\omega)\to g(\omega)$, since in such a range the dominant contribution is due to the silver ions.

The experiment was performed on the inelastic time-of-flight spectrometer IN6 at the Institute Laue-Langevin (Grenoble). The chosen wavelength for the incident beam was 5.12 Å (approximately 3.12 meV) and the instrumental resolution was about 0.1 meV (1 meV→11.6 K→8.06 $\rm cm^{-1}$). Due to its high absorption, the sample was put in the beam at an angle of 45°; this reduced the range of explorable exchanged momenta to high values, but increased substantially the signal-to-noise ratio on the high angle detectors. The data were binned in 37 spectra, 16 of which gave reliable results. The corresponding elastic Q-range explored was thus 1.304 to 2.046 $\rm Å^{-1}$.

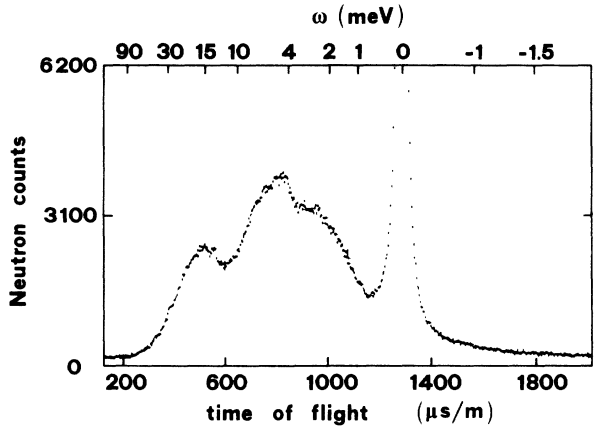

FIG. 2. Time-of-flight neutron-scattering spectrum of $x=0.65$ sample at 176 K.

Spectra were taken at three different temperatures (176, 232, and 288 K) for each sample. In Fig. 2 we show a typical time-of-flight spectrum of the $x=0.65$ sample at 176 K (in the following we shall use this sample and temperature to illustrate our results). After the standard calibration procedures by means of a Vanadium run, the empty-can contribution was subtracted and the absolute differential scattering cross section was determined. The elastic contribution was then identified and subtracted using a program which found the best fit to the data up to

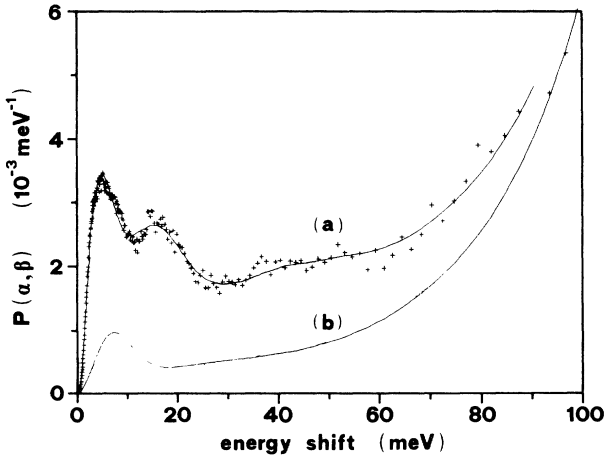

FIG. 3. Experimental $P(\alpha,\beta)$ (crosses) and best fit [solid line (a)] using the dynamical model and iterative procedure described in the text. Solid line (b) represents the calculated multiphonon contribution.

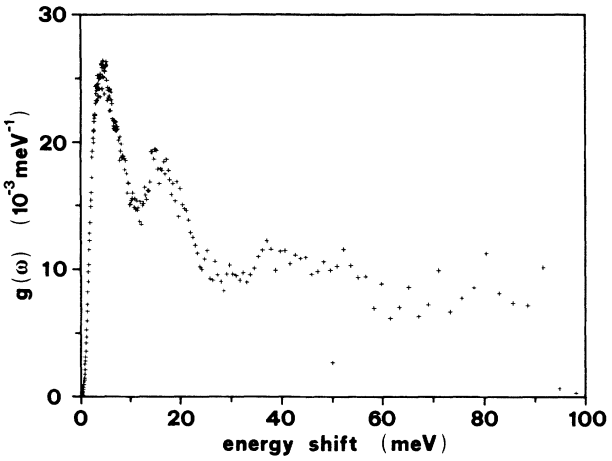

FIG. 4. Experimental vibrational density of states.

an energy transfer of 2 meV. In principle, this allowed us to explore the inelastic scattering down to 0.1 meV. At this point the experimental $P(\alpha,\beta)$ was obtained (see Fig. 3 for an example). Finally, the experimental density of states $g_N(\omega)$ was obtained using the following iterative procedure, which was chosen because our sample is mainly a coherent scatterer. Given a user-defined number of vibrational modes, characterized by 5 parameters each, i.e., the scatterer mass, the frequency, the intensity, the cutoff frequency, and the shape of the peak in the spectrum, the theoretical density of states was calculated. From this, both the Debye-Waller factor and the multiphonon contribution were estimated and used to evaluate a model $P(\alpha,\beta)$ which was fitted to the experimental one. The initial parameters were then varied until a satisfactory fit was achieved (see Fig. 3). At this point the procedure was inverted, and $g(\omega)$ was obtained after subtraction of the multiphonon contribution.

In our dynamical modeling we used four vibrational modes. We found that in order to be able to fit the low-frequency region, we had to assume that silver atoms *alone* were responsible for the lowest-frequency vibration. For the other modes instead the average mass of the borate glass formula unit was acceptable. In Fig. 4 we show the final $g_N(\omega) \rightarrow g(\omega)$.

Finally, the linear portions of the double-logarithmic plot of $g(\omega)$ obtained for each sample and temperature were interpolated with an interactive Minuit routine.

III. VIBRATIONAL RAMAN SCATTERING ON FRACTALS

In their original paper,[15] Alexander and Orbach point out the isomorphism between diffusion on a lattice and vibrational dynamics. If the lattice is a fractal structure, the scaling of the diffusion coefficient with distance (characterized by the exponent θ) will lead to quasilocalization of vibrational modes in the acoustic range. The density of such modes ("fractons") reflects the scaling behavior of the diffusion coefficient and will scale with frequency according to the law

$$g_{\rm fr}(\omega) \approx \omega^{\tilde{d}-1} . \tag{9}$$

It is evident that in a real system such a law will have upper (ω_f) and lower (ω_0) frequency cutoffs, respectively, related to lower (l_f) and upper (l_0) length cutoffs.[15] On the lowest length scale, that of the smallest interatomic separation, the vibrational density of states is dominated by optic modes, or in any case vibrations which are only sensitive to very-short-range order. More interesting is the upper length cutoff, which corresponds to the crossover from the anomalous fracton regime to the ordinary Debye range.[16] The detection of the corresponding crossover frequency ω_0 thus allows the determination of the spatial scale over which the system may be considered fractal; furthermore, from the scaling of ω_0 with l_0 the exponent θ may be determined, as shown experimentally by Fontana *et al.*[4]

In the specific case of superionic borate glasses, the fractal structure is supposed to be related to the distribution of AgI fourfold-coordinated units in the borate glass matrix. This would indicate that the lower cutoff distance $l_f \approx a$, where a is the Ag-I separation as determined by extended x-ray-absorption fine structure (EXAFS).[17] From the detection of the crossover frequency between fracton and Debye behavior, the upper cutoff distance l_0 was estimated to be in the range of 20 to 30 Å.[4] Thus, in principle, three ranges may be identified in the vibrational density of states: at the lowest frequencies (in our case up to ≈ 10 cm^{-1}) the Debye range where acoustic modes are expected to dominate $g(\omega)$, and hence

$$g(\omega) \approx \omega^{d-1} \equiv \omega^2 , \tag{10}$$

where $d=3$ is the Euclidean dimensionality. The intermediate range ($10 \leq \omega \leq 20$ cm^{-1}) is the crossover region, which may also be characterized by the so-called "fracton edge,"[16] or by an increase of bond-bending modes.[18] The upper end of this range is marked by ω_0, after which we find the anomalous fracton regime, where $g(\omega)$ should scale according to (9).

The possible existence of three separate ranges over a relatively small frequency interval (≈ 50 cm^{-1}) makes their experimental identification particularly difficult and somewhat ambiguous. More specifically, we refer to the definition of the crossover range and to the upper frequency cutoff of the fracton range. Thus the results we shall present, and in particular the value of the fracton dimensionality $\tilde{d}$, will be affected by an uncertainty which is larger than the random error to be expected from the quality of the data.

Now let us consider a vibrational mode of a fractal system;[3] we may assume that this mode will be localized by the disorder. In other words, the amplitude $u(r)$ of the mode γ (with energy $\hbar\omega_\gamma$) at position r will decay exponentially with r. Alexander *et al.* (1985) made the hypothesis that the wave function $\phi_\gamma(r)$ which is proportional to $u_\gamma(r)$ can be expressed by

$$\phi_\gamma(\omega_\gamma,L)\approx l_{\omega_\gamma}^{-d_f/2}\exp\left[-\frac{1}{2}\left[\frac{L}{l_{\omega_\gamma}}\right]^\delta\right], \quad (11)$$

where l_{ω_γ} is the localization length at the frequency $\omega=\omega_\gamma$, d_f is the fractal ($\approx$Hausdorff) dimension, L is the spatial variable, δ is the so-called superlocalization exponent which determines different decay shapes; for lack of better information on δ, in our work we make the simplest assumption putting $\delta=1$ [see also Duval *et al.* (1987)].

Furthermore,

$$l_{\omega_\gamma}\approx\omega^{-\tilde{d}/d_f}. \quad (12)$$

The intensity of light scattering $I(\omega)$ is proportional to the square of the polarizability changes, which are proportional to the displacement $\Delta x_{ik}(t)=\Delta x_i(t)-\Delta x_k(t)$ which, in turn, is proportional to $\nabla\phi(\omega,L)$. From Eqs. (11) and (12) we have

$$\nabla\phi\approx\omega^{\tilde{d}/d_f+\tilde{d}/2}\exp(-L/2l_{\omega_\gamma}). \quad (13)$$

Using the Fermi Golden rule we can calculate the transition probability per unit time $W(\omega_\gamma,L)$ for an electron to change its state to another one whose energy differs from that of the initial state by ω_γ because of the exchange of a fracton of the same energy localized about position L. By summing over all the possible fracton modes and by normalizing, we obtain for the light scattering intensity due to a Stokes process

$$I(\omega)\approx\omega^{[\tilde{d}/d_f(d_f+2)]-2}[n(\omega,T)+1], \quad (14)$$

where Eq. (9) for the fracton density of states was used. From Eq. (14) we deduce therefore that

$$C(\omega)\approx\omega^{2\tilde{d}/d_f}. \quad (15)$$

Fontana *et al.* (1987) used scaling from (15) with $d_f=d$, since they assumed the coexistence of finite clusters of AgI coordinated groups with the infinite cluster. However, up to now no direct experimental evidence was available to confirm such hypotheses and calculations. By taking the ratio of $I_R(\omega)$ obtained by Raman spectroscopy to $g(\omega)$ determined by inelastic neutron scattering, the coupling function may be determined directly in the frequency range of interest here.

IV. RESULTS AND DISCUSSION

A. The density of states

The Raman data confirm our previously reported results.[4] For instance, in Fig. 5(a) we show the reduced Raman intensity for the $x=0.65$ sample at 176 K. As stated, this is the experimental quantity which we use to determine the coupling $C(\omega)$. In Fig. 5(b) we show the double logarithmic plot of $I_R(\omega)$ versus ω; we note the clear evidence of the crossover between the Debye and the fracton range, as already shown in Ref. 4.

Coming now to neutron scattering, we first remark that only by assuming that at low frequencies only silver ions

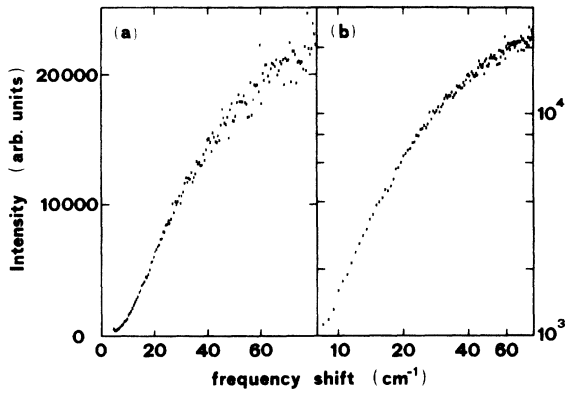

FIG. 5. (a) Reduced Raman intensity of $x=0.65$ sample; (b) Double logarithmic plot of $I_R(\omega)$.

contribute to the density of states could we fit reasonably well the experimental $P(\alpha,\beta)$ (Fig. 3). This result, coupled to previous Raman data,[9] confirms that at low frequencies the major contribution to the spectra is due to the motion of the silver atoms, and more specifically those belonging to the AgI tetrahedra.

With this in mind, let us consider the behavior of the experimental density of states. In Fig. 6 we show a double-logarithmic plot of $g(\omega)$ versus ω, again for the $x=0.65$ sample at 176 K. In the figure, the three spectral ranges discussed in the preceding paragraph are marked. The solid lines are the best fit to the identifiable linear portions using least-squares routines. In Fig. 7 we show these specific spectral ranges in detail. The analysis was performed on all samples and temperatures, and the results for the slopes of the linear portions are summarized in Table I.

The Debye range is clearly identified by the exponent values close to 2, obtained for all samples. The errors

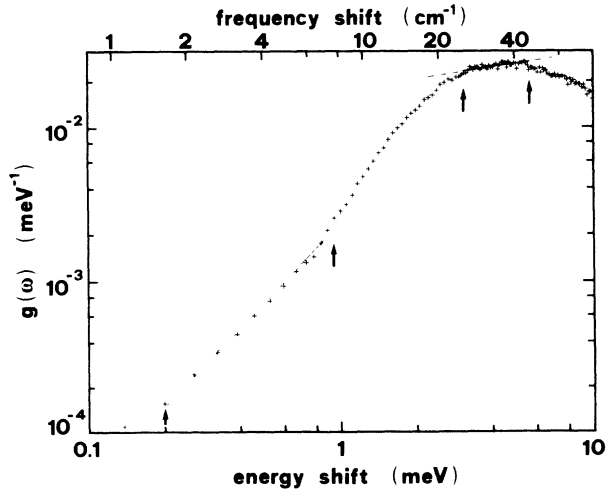

FIG. 6. Double-logarithmic plot of $g(\omega)$ for the $x=0.65$ sample at 176 K.

TABLE I. Values of scaling exponents of the density of states in the Debye (upper number) and fracton (lower number) ranges.

T	$x=0.40$	$x=0.55$	$x=0.65$
176 K	1.66±0.08	1.67±0.08	1.74±0.08
	0.28±0.03	0.49±0.03	0.27±0.03
232 K	1.68±0.08	1.66±0.08	1.65±0.08
	0.50±0.03	0.32±0.03	0.16±0.03
288 K	1.64±0.18	1.72±0.18	1.70±0.18
	0.64±0.04	0.50±0.03	0.25±0.03

quoted in Table I are those of the least-squares routine; the real error, however, is expected to be larger, probably by as much as a factor of 3. This is due to the complex procedure necessary to obtain $g(\omega)$. We also note that

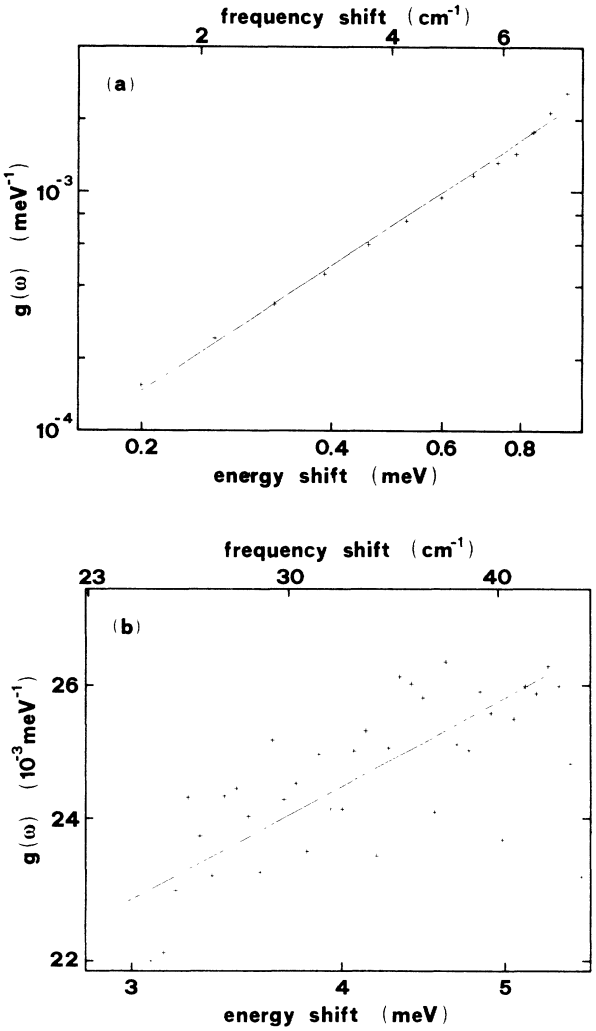

FIG. 7. Linear portion of the data of Fig. 6 in expanded scale: (a) Debye range; (b) fracton range. The solid line is a least-squares best fit.

there is a systematic deviation from the Debye line of the lowest-frequency points, particularly at high temperature. Although our procedure parametrizes and subtracts the elastic and quasielastic portion of the scattered intensity, it is clear that a small error in such subtraction could yield large deviations in the observed $g(\omega)$. Such an error would be expected to decrease as temperature decreases, and in fact the deviation is much smaller in the data at 176 K. By such considerations we might justify the small but seemingly systematic deviation of the Debye exponent from the theoretical value of 2. However, at this point we may recall the similar result obtained for the Debye range in amourphous silica by Buchenau *et al.*,[19] which was interpreted as due to the coexistence of localized modes with the ordinary acoustic waves. It would be entirely reasonable that this could be the case for our samples also. Thus we feel justified in assigning the first linear range to the Debye part of $g(\omega)$. Let us also note that this zone extends up to ≈ 8 cm^{-1} (1 meV) for all samples studied and for all temperatures. This independence on sample and temperature confirms the identification of the Debye range, which should not be too sensitive to variations in the details of the local ordering.

The other linear range in $g(\omega)$ identifies the anomalous fracton regime, above the fracton edge which itself terminates at the crossover frequency ω_0. In this range the noise level is much higher and therefore the errors both in the exponent and in the identification of the range itself are larger. In analyzing the data in this region, two independent procedures were followed. The first, more automatic, let the linear portion be selected by the Minuit fitting routine, using its confidence and correlation parameters as indicators of the best straight line. The resulting values of the exponents and the errors quoted in Table I refer to this procedure. The other method consisted of choosing what would appear to be a good fracton range by inspection, and then using the least-square routine to obtain the exponent values. We found to our satisfaction that both approaches yielded remarkably similar results, thus removing some of the obvious ambiguity in trying to identify and fit a power law to the fraction region. As expected, the fracton exponents are affected by a larger relative error than the Debye exponents. Also as expected, however, this error seems to be less systematic in character. Thus we tend not to assign much significance to the different values of the exponents we found for different samples and temperatures, and therefore quote an average value of 0.4±0.1 for the fracton exponent. This would correspond to a fracton dimensionality of $\tilde{d} \approx 1.4$, in good agreement with the value predicted for a three-dimensional percolation network.[15]

B. The coupling function

In Fig. 8 we show the ratio $I_R(\omega)/g(\omega)$ which, according to the previous discussion, should approximate well the functional dependence of $C(\omega)$, especially in the low-frequency range. Confining now our analysis to this region, we first note that $C(\omega)$ tends to a constant value at

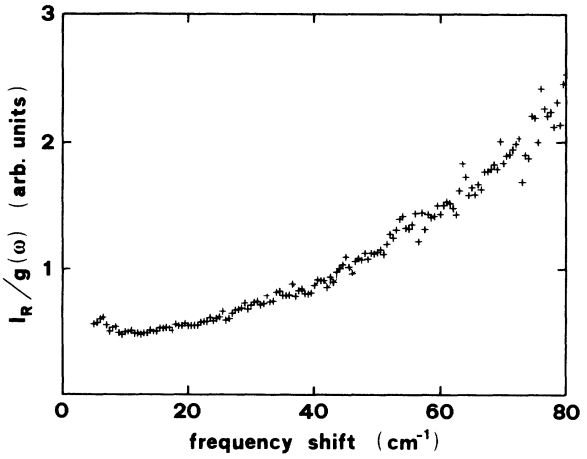

FIG. 8. Ratio of $I_R(\omega)$ to $g(\omega)$.

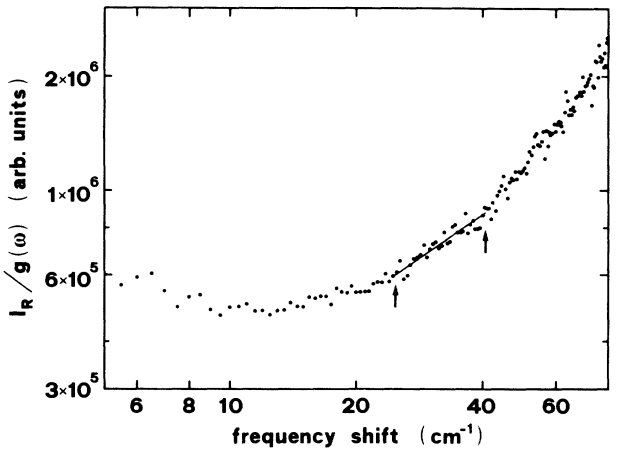

FIG. 9. Double-logarithmic plot of $C(\omega)$.

very low frequencies. The final rise for $\omega\rightarrow 0$ is connected with the quasielastic part of Raman scattering, as shown by its sharp increase with increasing temperature. At 80 K, $C(\omega)$ is practically flat down to the lowest frequency probed by our experiments. This is shown more clearly in the double-logarithmic plot of Fig. 9. It is important to note that $C(\omega)\approx$const in the Debye range, where instead a parabolic dependence on ω is expected. Here we might remark that on a linear scale $C(\omega)$ might look similar to a parabola; however, this is not so, as shown in Fig. 9. At this time it would be premature to try and give a quantitative interpretation of such behavior. We feel that the constancy of $C(\omega)$ at very low frequencies should be confirmed by further, more precise measurements in this difficult range. With this in mind, however, we feel that the deviation of $C(\omega)$ from the expected ω^2 behavior may indicate localization in the electronic states (let us not forget that Raman scattering is connected to local fluctuations of atomic or molecular polarizability) due to the locally disordered structure of dissolved AgI.

The other interesting feature of $C(\omega)$ is its scaling behavior in the fracton range, as shown by the linear fit (solid line in Fig. 9). To our knowledge this is the first experimental evidence of such behavior. The scaling exponent is independent of temperature and sample, and its average value is ≈ 0.84. Using Eq. (15) and the value $\tilde{d}=1.4$ obtained from $g(\omega)$, we would predict 0.9, which is satisfyingly close to the directly measured value. Thus our data confirm rather well the validity of the assumptions and calculations leading to scaling law (15) for the electron-vibration coupling function in a microscopic fractal.

V. CONCLUSIONS

AgI-doped silver borate glasses have turned out to be interesting not only for their superionic transport properties but also as sample systems to study the dynamical consequences of fractality over length scales of the order of tens of angstroms. Although it is true that the fractality of a system may not be proved by dynamics alone,[20] we feel that the values of the scaling exponents we have obtained and their internal consistency are strong experimental evidence in favor of dynamic fractality in the silver borate system. This evidence is further strengthened by the anomalous temperature dependence of the specific heat[21] and by recent neutron-diffraction experiments.[22] An interesting open question (apart from a more precise determination of the Ag local environment by EXAFS and diffraction experiments) is whether fractality persists at low silver iodide concentrations. Although the previous Raman data[4] seemed to imply that it did not, the neutron-scattering data presented here show dynamical fractality for the $x=0.4$ sample also. Thus a more careful study of this system on the low concentration side of AgI content would be quite useful, not only to address the problem of dynamics versus structural fractality, but also to investigate whether at least some kind of fractality might not be a general property of the glassy state.

ACKNOWLEDGMENTS

We wish to thank Dr. A. Tomasi for preparing and characterizing the samples.

[1]See, for instance, B. B. Mandelbrot, *The Fractal Geometry of Nature* (Freeman, San Francisco, 1982).

[2]R. Orbach, J. Stat. Phys. **36**, 375 (1984); R. Rammal, *ibid.* **36**, 547 (1984).

[3]S. Alexander, O. Entin-Wohlman, and R. Orbach, Phys. Rev. B **32**, 6447 (1985); A. Aharony, S. Alexander, O. Entin-Wohlman, and R. Orbach, Phys. Rev. Lett. **58**, 132 (1987); see also E. Duval, G. Mariotto, M. Montagna, O. Pilla, G. Viliani, and M. Barland, Europhys. Lett. **3**, 333 (1987).

[4]A. Fontana, F. Rocca, and M. P. Fontana, Phys. Rev. Lett. **58**, 503 (1987).

[5]G. Maisano, P. Migliardo, M. P. Fontana, M. C. Bellissent-

Funel, and A. J. Dianoux, J. Phys. C **18**, 1115 (1985).
[6]A. J. Dianoux, J. N. Page, and H. M. Rosenberg, Phys. Rev. Lett. **58**, 886 (1987).
[7]T. Freltoft, J. Kjems, and D. Richter, Phys. Rev. Lett. **59**, 1212 (1987).
[8]A. Magistris, G. Chiodelli, and A. Schiraldi, Electrochim. Acta **24**, 203 (1979).
[9]A. Fontana, G. Mariotto, and F. Rocca, Phys. Status Solidi B **129**, 489 (1985); A. Fontana and F. Rocca, Phys. Rev. B **36**, 9279 (1987).
[10]For general reviews, see M. H. Brodsky, in *Light Scattering in Solids,* edited by M. Cardona (Springer, Berlin, 1975); D. I. Wearie, in *Amorphous Solids,* edited by W. A. Phillips (Springer, Berlin, 1981).
[11]F. L. Galeneer and P. N. Sen, Phys. Rev. B **17**, 1928 (1978).
[12]R. J. Nemanich, Phys. Rev. B **16**, 1665 (1977); see, however, G. A. Connell, Phys. Status Solidi B **69**, 9 (1975).
[13]See, for instance, W. Marshall and S. W. Lovesey, *Theory of Thermal Neutron Scattering* (Oxford University Press, London, 1971).
[14]P. A. Egelstaff and P. Schofield, Nucl. Sci. Eng. **12**, 260 (1962).
[15]S. Alexander and R. Orbach, J. Phys. (Paris) Lett. **43**, L625 (1982).
[16]A. Aharoni, S. Alexander, O. Entin-Wohlman, and R. Orbach, Phys. Rev. B **31**, 2565 (1985); S. Alexander, C. Laermans, R. Orbach, and H. M. Rosenberg, *ibid.*, **28**, 4615 (1983).
[17]F. Rocca, G. Dalba, and P. Fornasini, Mater. Chem. Phys. **23**, 85 (1989).
[18]Shechao Feng, Phys. Rev. B **32**, 5793 (1985).
[19]U. Buchenau, M. Prager, N. Nucker, A. J. Dianoux, N. Ahmad, and W. A. Phillips, Phys. Rev. B **34**, 5665 (1986).
[20]J. A. Krumhansl, Phys. Rev. Lett. **56**, 2696 (1986).
[21]A. Avogadro, S. Aldrovandi, and F. Borsa, Phys. Rev. B **33**, 5637 (1986).
[22]L. Borjesson, L. M. Torell, and W. S. Howells, Philos. Mag. B **59**, 105 (1989).